https://doi.org/10.20965/ijat.2018.p0024

Paper:

Graphene Nanomechanical Resonator Mass Sensing of Mixed H_2/Ar Gas

Manoharan Muruganathan[*,†], **Fumihiro Seto**[*], **and Hiroshi Mizuta**[*,**]

[*]School of Material Science, Japan Advanced Institute of Science and Technology
Nomi 923-1211, Japan
[†]Corresponding author, E-mail: mano@jaist.ac.jp
[**]Hitachi Cambridge Laboratory, Cambridge, United Kingdom
[Received June 1, 2017; accepted November 23, 2017]

We report the local top-gated graphene resonator inertial mass sensing of mixed H_2/Ar gas. The graphene resonator is fabricated with monolayer graphene. The fabricated resonator dimensions are 900 nm in length and 500 nm in width. Measurements of the fabricated resonator are performed using a co-planar structure probe and radio-frequency (RF) connectors. At the vacuum condition of the chamber, the resonant frequency of the doubly clamped graphene resonator is measured as 94.3 MHz with the quality factor of 42.2, based on transmission S-parameter characterization. The measured resonant frequency is consistent with the theoretical calculation based on the continuum model for the graphene resonator. When the chamber pressure is increased to 1.1×10^{-1} Pa by injecting mixed H_2/Ar gas, the resonant frequency of the device is downshifted by 4.32 MHz to 89.98 MHz and the quality factor is reduced to 22.5. As the mass of the graphene resonator is increased by the adsorption of mixed gas molecules adsorption, the resonant frequency is downshifted further. The detected mass of the adsorbed gas molecules is calculated as $\sim$15 attograms.

Keywords: graphene, NEMS, resonator, inertial mass sensing

1. Introduction

Graphene is a promising two-dimensional (2D) material candidate for gas sensing because of its ultralow thickness and excellent electronic properties [1, 2]. Moreover, graphene has the largest sensing area per unit volume of any solid material. Furthermore, because of its high-quality crystal lattice, graphene has an ultra-high Young's modulus of 1 TPa. This unique property indicates the potential of graphene as a candidate for future nanoelectromechanical systems (NEMS) applications [3–5]. With these unique advantages, graphene-based NEMS are highly sensitive to environmental changes in terms of their electrical and mechanical characteristics [6, 7]. Graphene-based NEMS devices have been proposed for highly sensitive mass detection of neutral species; significant progress has been made in sensing heavy molecules such as protein bovine serum albumin, pentacene, and β-amylase [8, 9]. Carbon nanotube resonators have been used to measure the yoctogram-level mass of naphthalene molecules [10] and SiC resonators are used to measure the zeptogram-level mass of Xe atoms [11]. All NEMS resonator mass-sensing studies have focused on sensing relatively heavy molecules. However, mass sensing of lightweight gas molecules with mass sensors has not been well explored. Other device architectures are used for low-molecular-weight molecules such as H_2, CH_4, etc. [12].

Sensing of very lightweight molecules like H_2 will permit individual molecular mass spectroscopy in a single graphene-based NEMS resonator device. All reported graphene-based resonator works have been based on global back gate operation. The local top gate geometry may permit more localized operation of the RF signal, rather than exciting the entire device. However, the local top gate geometry may also block the path of molecules to a very small area of resonator.

In this research, we report on a local top-gated graphene resonator used in the mass sensing of lightweight mixed H_2/Ar gas molecules. Here, we demonstrate that double-clamped graphene nanoribbon resonators are capable of attogram-level mass sensing of lightweight gas molecules.

2. Device Fabrication and RF Measurement Setup

2.1. Fabrication of Suspended Graphene Resonator Device

We used chemical vapor deposition (CVD) graphene from Graphene Platform Corp. for the resonator fabrication. The substrate size is 10 mm $\times$ 10 mm, and the thickness of SiO_2 is 285 nm. **Fig. 1** shows the Raman spectra of the transferred CVD graphene on to SiO_2/silicon substrate at three different locations. The G peak at $\sim$ 1580 cm^{-1} and the 2D peak at $\sim$ 2700 cm^{-1} are observed in all three positions. The significantly weak D peak ($\sim$ 1350 cm^{-1}) and the shape of the 2D peak indicate the

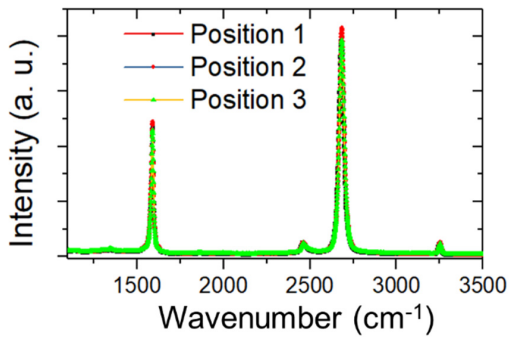

Fig. 1. Raman spectra of CVD graphene on SiO_2/Si substrate at three different positions.

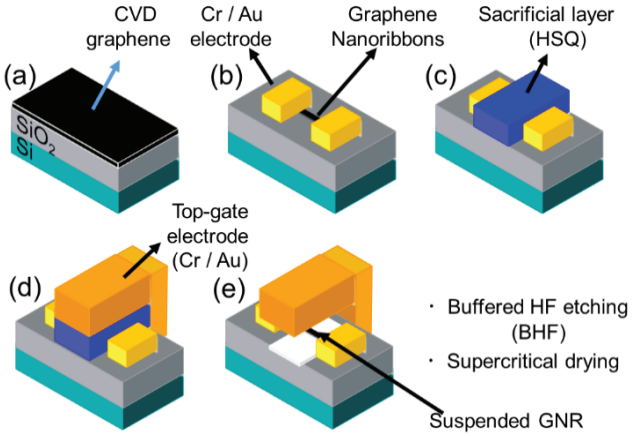

Fig. 2. Schematics of Device fabrication processes: (a) CVD graphene on Si substrate with 285 nm SiO_2 layer (b) GNR patterning and contact electrode fabrication processes (c) Fabrication of sacrificial layer (HSQ resist) on graphene nanoribbon (d) Top gate electrode fabrication step (e) Fabrication of suspended structure using BHF etching and supercritical point drying.

monolayer nature of the CVD graphene [13]. **Fig. 2** shows the device fabrication processing steps. First, we pattern graphene nanoribbons (GNR) using electron-beam lithography (EBL) and reactive-ion etching (RIE). 10-W O_2 plasma was used in RIE etching at a pressure of 4 Pa for 10 s. The size of GNR is 900 nm in length and 500 nm in width. After that, the GNR is connected to Cr/Au (5/80 nm) electrodes on a substrate by EBL, electron beam evaporation, and lift-off processes (**Fig. 2(b)**). Next, we prepare a sacrificial layer (80 nm) on GNR by EBL using H-silsesquioxane (HSQ), which is a negative-type resist (**Fig. 2(c)**). The HSQ resist is converted to an SiO_2 layer after electron-beam exposure in the EBL step [14, 15]. Thereafter, a top-gate electrode (Cr/Au = 5/140 nm, 2000 nm in width, 180 nm in length) is fabricated on the sacrificial layer (**Fig. 2(d)**). In order to reduce the defects in the GNR, annealing was performed in H_2 gas [16, 17]. Finally, the sacrificial layer of SiO_2 and the SiO_2 beneath the GNR are selectively removed by buffered HF etching (BHF: HF:NH_4F: 1:6), and supercritical drying is used to realize suspended GNR (**Fig. 2(e)**).

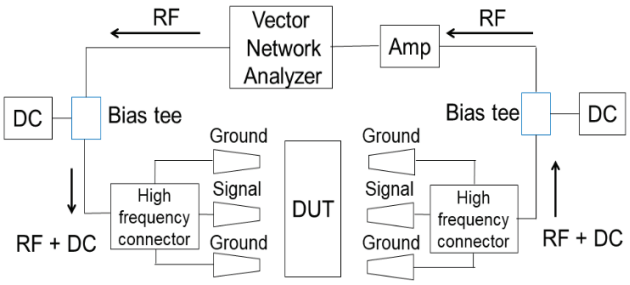

Fig. 3. Radio frequency (RF) measurement setup schematic depicting co-planar waveguide probes and other RF components for resonant characteristics measurements.

The optical microscope image of the fabricated device is shown in **Fig. 5(a)**.

2.2. Device Measurement Conditions

The fabricated device is characterized by the following two different sets of measurements: a) resonant frequency measurement of doubly clamped GNR in vacuum (pressure: 1.1×10^{-4} Pa), and b) Measurement of resonant frequency in mixed H_2/Ar (9:1) gas at pressure of 1.1×10^{-1} Pa.

2.2.1. Resonant Frequency Measurement of Doubly Clamped GNR

The resonant frequency of the device is measured using a high-frequency measurement setup. The measurement circuit diagram is shown in **Fig. 3**. Measurement was performed using a vector network analyzer (VNA), bias tee, ground-signal-ground (GSG) co-planar structure probe for high-frequency measurement, and an RF amplifier. The RF signal from the VNA is combined with a DC voltage in the bias tee and then sent to the gate terminal of the graphene resonator (**Fig. 2(e)**, top gate). This signal is used to excite the resonator at different RF frequencies. The drain terminal of resonator is biased with another DC source and a bias tee as shown in the right side of **Fig. 3**. The transmitted signal from the resonator is measured at the VNA. The amplitude and phase of the S_{21} parameter are also measured at VNA. All RF signal paths are connected using high-frequency cables and Sub-Miniature version A (SMA) connectors. Co-planar structured probes, connectors, and the device itself are held in a vacuum chamber. The source terminal is grounded in all measurements. The co-planar transmission line is used for the RF terminals of the resonator, i.e., the gate and drain electrodes.

2.2.2. Measurement of Resonant Frequency in 9:1 Ar/H_2 Gas Environment

The mixed 9:1 Ar/H_2 gas was introduced into the vacuum chamber through a mass flow controller. The pressure of the chamber was monitored to determine changes in the chamber gas environment.

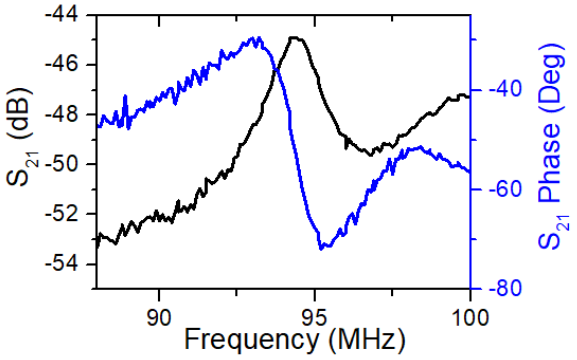

Fig. 4. Measured transmission S-parameter characteristics of doubly clamped graphene resonator in vacuum condition (1.1×10^{-4} Pa).

3. Results & Discussion

Characterization of the doubly clamped graphene resonator is an important step for the resonator design and the interpretation of the experimental results. To estimate the resonant frequency, the continuum model is used, which considers the graphene resonators as membranes with zero bending stiffness [8]. Based on this model, the resonant frequency at zero gate voltage is given by

$$f_{res} = \frac{1}{2L}\sqrt{\frac{T_0}{\rho W}} \quad \ldots\ldots\ldots\ldots\ldots\ldots \quad (1)$$

where L and W are the length and width of the doubly clamped graphene beam, respectively. $\rho = 7.4 \times 10^{-19}$ kg/μm^{-2} is the two-dimensional mass density of graphene. The built-in tension of the graphene resonator T_0 is 13 nN [18]. For our resonator dimensions, the resonant frequency is calculated as 104.13 MHz.

Figure 4 shows the high-frequency measurement results of the transmission S-parameter S_{21} in vacuum. The black line represents the magnitude of the resonance, and the blue line represents the phase response around the resonant characteristics. By this measurement, the resonance peak (f_0) is observed at 94.3 MHz. The quality factor (Q) is estimated as 42.2 from the 3-dB bandwidth of the resonant characteristics. Moreover, the resonant peak is 5 dB above the background signal. The phase characteristics change around the resonant peak, indicating inductive and capacitive reactance cancellation at the resonant peak.

This resonant frequency is almost consistent with the continuum model calculation given by Eq. (1). The slight deviation from the theoretical prediction of the resonant frequency is attributed to the over-etching of SiO_2 layer under GNR. Diffusion of HF along the graphene–oxide interface occurs quickly, a feature unique to graphene NEMS fabrication. This causes nearly uniform and over-etching of the SiO_2 underneath the graphene [19], as depicted in **Fig. 5**. This over-etching weakens the GNR anchor fixing, which may effectively increase the resonator length, as the clamping electrodes are also suspended. These factors affect the measured resonant frequency and Q factor of the resonator. Moreover, our graphene resonator is fabricated using CVD graphene, which can contain point defects, grain boundaries, and edge irregularities [20, 21]. These defects may also affect the mechanical and electrical characteristics of the resonator.

As a next step to realize the inertial mass sensing of gas molecules, we measured the transmission characteristics of the resonator in the presence of Ar + H_2 mixture (9:1) gas at 1.1×10^{-1} Pa. **Fig. 6** shows the measurement results of the resonance magnitude and the changes in the phase characteristics when the mixed Ar + H_2 gas is introduced. The black and red lines represent the resonance characteristic at the pressures of 1.1×10^{-4} and 1.1×10^{-1} Pa in the chamber, respectively. The resonant frequency of the device is downshifted by 4.32 MHz from the adsorption of the mixed gas molecules. Consequently, the Q factor is also reduced from 42.2 to 22.5 based on 3-dB bandwidth calculation. The resonance peak shifts and broadens as the gas molecules are adsorbed on the GNR surface. Furthermore, the resonant peak amplitude decreases. The presence of gas molecules may degrade the Q-factor via an increase in the material damping caused by surface molecular adsorption [22] and air damping from resonator–gas interactions [23]. Based on the harmonic oscillator picture [24], the vibrating GNR resonator should follow the relation of

$$\Delta f_0 = \frac{\Delta m}{2m_{GNR}} f_0 \quad \ldots\ldots\ldots\ldots\ldots\ldots \quad (2)$$

where f is the resonant frequency, Δf_0 is the shifted value of the resonance peak, Δm is the change in mass of GNR after molecular adsorption, and m_{GNR} is the effective mass of the GNR. From the measured values of the resonant frequency and frequency shift, the total mass detected is $\sim$ 15 attograms. First-principles simulations with the van der Waals exchange correlation functionals showed the binding energy of Ar [25] atoms and H_2 [26] molecules on graphene of 100 and 48 meV, respectively. Compared with the room-temperature thermal energy of $\sim$ 26 meV, these binding energies are clearly higher. As the binding energy and molecular concentration are higher for Ar, more Ar molecules might be adsorbed on the GNR. Our resonator's room-temperature Q-factor matches with the reported work of ref. [8], where the mass sensitivity of $\sim$ 2 zg is estimated for a graphene resonator. At 1.1×10^{-1} Pa, $\sim 2 \times 10^{18}$ molecules is introduced into the chamber. If we consider the number of Ar atoms contained in a 15-attogram mass, the number $\sim 2.2 \times 10^5$ is obtained. This number is reasonable, compared to the reported accretions of $\sim 2.3 \times 10^6$ Xe atoms on an SiC resonator surface area of 2.3 μm $\times$150 nm [11].

4. Conclusion

In this research work, we present a CVD graphene resonator with a local top gate for the mass sensing of mixed H_2/Ar gas. RF measurements of the resonator were performed using a co-planar structure probe and

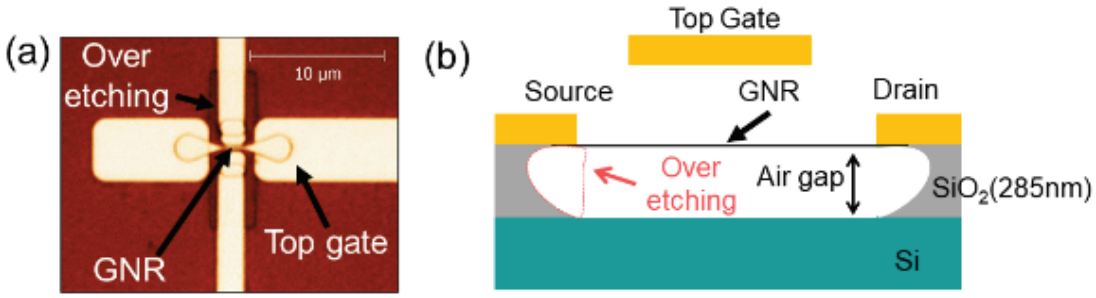

Fig. 5. (a) Optical microscope image of the fabricated graphene resonator. BHF over-etching is clearly visible as a trench. (b) Schematic depicting BHF over-etching in cross-sectional view and hanging of GNR resonator edges.

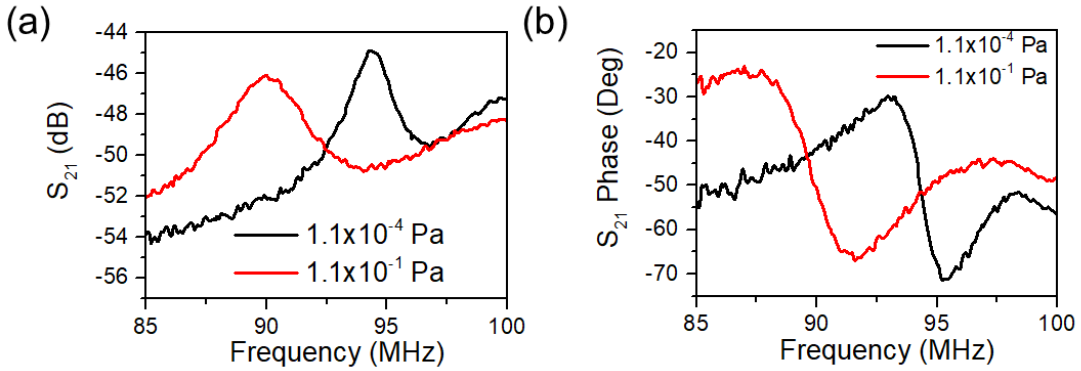

Fig. 6. Measurement results of transmission S-parameter characteristics of doubly clamped graphene resonator in Ar + H_2 (9:1) mixture gas at the different pressures of 1.1×10^{-4} Pa and 1.1×10^{-1} Pa. (a) Amplitude and (b) Phase characteristics of the measured S_{21} parameters.

RF connectors. The intrinsic characterization of the doubly clamped graphene resonator showed the resonant frequency of 94.3 MHz and Q-factor of 42.2 based on the 3-dB bandwidth calculation. The theoretically calculated resonant frequency based on the continuum model is consistent with the measured resonant frequency. In order to sense the H_2/Ar gas mixture, the chamber pressured was increased to 1.1×10^{-1} Pa by injecting the gas mixture, which downshifted the resonant frequency to 89.98 MHz and reduced the Q factor to 22.5. These measured results indicated the adsorption of the mixed gas molecules by the local top-gated graphene resonator; the mass of these adsorbed molecules was found to be $\sim$ 15 attograms. These results clearly indicate that the inertial mass of lightweight molecules can be sensed by a graphene nanoelectromechanical resonator.

Acknowledgements

This research has been funded through the Grant-in-Aid for Scientific Research (S) No. 25220904, Challenging Exploratory Research No. 16K13650, and Young Scientists (B) No. 16K18090.

References:

[1] K. S. Novoselov, "Electric Field Effect in Atomically Thin Carbon Films," Science, Vol.306, No.5696, pp. 666-669, 2004.
[2] F. Schedin, et al., "Detection of individual gas molecules adsorbed on graphene," Nat. Mater., Vol.6, No.9, pp. 652-655, 2007.
[3] M. Manoharan, T. Chikuba, N. Kanetake, J. Sun, and H. Mizuta, "Low pull-in voltage graphene nanoelectromechanical switches," 2015 Silicon Nanoelectronics Workshop (SNW), pp. 1-2, 2015.
[4] J. Sun, W. Wang, M. Muruganathan, and H. Mizuta, "Low pull-in voltage graphene electromechanical switch fabricated with a polymer sacrificial spacer," Appl. Phys. Lett., Vol.105, No.3, p. 033103, 2014.
[5] J. Sun, M. E. Schmidt, M. Muruganathan, H. M. H. Chong, and H. Mizuta, "Large-Scale Nanoelectromechanical Switches Based on Directly Deposited Nanocrystalline Graphene on Insulating Substrates," Nanoscale, 2016.
[6] M. Muruganathan, J. Sun, T. Imamura, and H. Mizuta, "Electrically Tunable van der Waals Interaction in Graphene–Molecule Complex," Nano Lett., Vol.15, No.12, pp. 8176-8180, 2015.
[7] J. Sun, M. Muruganathan, and H. Mizuta, "Room temperature detection of individual molecular physisorption using suspended bilayer graphene," Sci. Adv., Vol.2, No.4, pp. e1501518-e1501518, 2016.
[8] C. Chen et al., "Performance of monolayer graphene nanomechanical resonators with electrical readout," Nat. Nanotechnol., Vol.4, No.12, pp. 861-867, 2009.
[9] C. Chen et al., "Graphene mechanical oscillators with tunable frequency," Nat. Nanotechnol., Vol.8, No.12, pp. 923-927, 2013.
[10] J. Chaste, A. Eichler, J. Moser, G. Ceballos, R. Rurali, and A. Bachtold, "A nanomechanical mass sensor with yoctogram resolution," Nat. Nanotechnol., Vol.7, No.5, pp. 301-304, 2012.
[11] Y. T. Yang, C. Callegari, X. L. Feng, K. L. Ekinci, and M. L. Roukes, "Zeptogram-Scale Nanomechanical Mass Sensing," Nano Lett., Vol.6, No.4, pp. 583-586, 2006.
[12] Y. Fukushima, T. Suzuki, K. Onda, H. Komatsu, H. Kuroiwa, and T. Kaburagi, "Study on the Online Monitoring of Burn Marks by Gas Sensor," Int. J. Autom. Technol., Vol.11, No.1, pp. 112-119, 2017.
[13] D. Parobek, G. Shenoy, F. Zhou, Z. Peng, M. Ward, and H. Liu, "Synthesizing and Characterizing Graphene via Raman Spectroscopy: An Upper-Level Undergraduate Experiment That Exposes Students to Raman Spectroscopy and a 2D Nanomaterial," J. Chem. Educ., Vol.93, No.10, pp. 1798-1803, 2016.
[14] A. E. Grigorescu and C. W. Hagen, "Resists for sub-20-nm electron beam lithography with a focus on HSQ: state of the art," Nanotechnology, Vol.20, No.29, p. 292001, 2009.

[15] B. Kaleli, A. A. I. Aarnink, S. M. Smits, R. J. E. Hueting, R. A. M. Wolters, and J. Schmitz, "Electron beam lithography of HSQ and PMMA resists and importance of their properties to link the nano world to the micro world," 2010.
[16] T. Iwasaki et al., "Hydrogen intercalation: An approach to eliminate silicon dioxide substrate doping to graphene," Appl. Phys. Express, Vol.8, No.1, p. 015101, 2015.
[17] T. Iwasaki, M. Muruganathan, M. E. Schmidt, and H. Mizuta, "Partial hydrogenation induced interaction in a graphene–SiO_2 interface: irreversible modulation of device characteristics," Nanoscale, Vol.9, No.4, pp. 1662-1669, 2017.
[18] J. S. Bunch et al., "Electromechanical Resonators from Graphene Sheets," Science, Vol.315, No.5811, pp. 490-493, 2007.
[19] E. Stolyarova et al., "Observation of Graphene Bubbles and Effective Mass Transport under Graphene Films," Nano Lett., Vol.9, No.1, pp. 332-337, 2009.
[20] M. Manoharan and H. Mizuta, "Point defect-induced transport bandgap widening in the downscaled armchair graphene nanoribbon device," Carbon, Vol.64, pp. 416-423, 2013.
[21] M. Manoharan and H. Mizuta, "Edge irregularities in extremely down-scaled graphene nanoribbon devices: role of channel width," Mater. Res. Express, Vol.1, No.4, p. 045605, 2014.
[22] S. Joshi, S. Hung, and S. Vengallatore, "Design strategies for controlling damping in micromechanical and nanomechanical resonators," EPJ Tech. Instrum., Vol.1, No.1, pp. 1-14, 2014.
[23] J. Lee, Z. Wang, K. He, J. Shan, and P. X.-L. Feng, "Air damping of atomically thin MoS 2 nanomechanical resonators," Appl. Phys. Lett., Vol.105, No.2, p. 023104, 2014.
[24] H.-Y. Chiu, P. Hung, H. W. C. Postma, and M. Bockrath, "Atomic-Scale Mass Sensing Using Carbon Nanotube Resonators," Nano Lett., Vol.8, No.12, pp. 4342-4346, 2008.
[25] J. Kysilka, M. Rubeš, L. Grajciar, P. Nachtigall, and O. Bludský, "Accurate Description of Argon and Water Adsorption on Surfaces of Graphene-Based Carbon Allotropes," J. Phys. Chem. A, Vol.115, No.41, pp. 11387-11393, 2011.
[26] F. Costanzo, P. L. Silvestrelli, and F. Ancilotto, "Physisorption, Diffusion, and Chemisorption Pathways of H 2 Molecule on Graphene and on (2,2) Carbon Nanotube by First Principles Calculations," J. Chem. Theory Comput., Vol.8, No.4, pp. 1288-1294, 2012.

Name:
Manoharan Muruganathan

Affiliation:
Senior Lecturer, School of Materials Science, Japan Advanced Institute of Science and Technology (JAIST)

Address:
1-1 Asahidai, Nomi, Ishikawa 923-1292, Japan

Brief Biographical History:
2008, Ph.D in Physical Electronics from Tokyo Institute of Technology
2008-2012 Assistant Professor in IIITDM, Kancheepuram, India
2012-2017 Assistant Professor, Japan Advanced Institute of Science and Technology (JAIST)

Main Works:
• M. Manoharan, et al., "Silicon-on-insulator-based radio frequency single-electron transistors operating at temperatures above 4.2 k," Nano letters, Vol.8, No.12, pp. 4648-4652, 2008.
• M. Manoharan et al., "Electrically Tunable van der Waals Interaction in Graphene-Molecule Complex," Nano letters, Vol.15, No.12, pp. 8176-8180, 2015.

Membership in Academic Societies:
• Japan Society of Applied Physics (JSAP)
• American Chemical Society (ACS)

Name:
Fumihiro Seto

Affiliation:
Student, School of Materials Science, Japan Advanced Institute of Science and Technology (JAIST)

Address:
1-1 Asahidai, Nomi, Ishikawa 923-1292, Japan

Brief Biographical History:
2012 Associate degree in Electrical Engineering from National Institute of Technology, Kushiro College
2014 Bachelor in Electronic Information System Engineering from National Institute of Technology, Kushiro College
2017 Master in Material Science from Japan Advanced Institute of Science and Technology

Membership in Academic Societies:
• Japan Society of Applied Physics (JSAP)

Name:
Hiroshi Mizuta

Affiliation:
Professor, School of Materials Science, Japan Advanced Institute of Science and Technology (JAIST)

Address:
1-1 Asahidai, Nomi, Ishikawa 923-1292, Japan

Brief Biographical History:
1993 Ph.D in Engineering from Osaka University
1997-2003 Laboratory Manager and Senior Researcher, Hitachi Cambridge Laboratory, UK
2003-2007 Associate Professor, Tokyo Institute of Technology
2007-2016 Professor of Nanoelectronics, University of Southampton
2011- Professor, JAIST
2017- Distinguished Professor
2017- Visiting Chief Scientist, Hitachi Cambridge Laboratory

Main Works:
• "The Physics and Applications of Resonant Tunnelling Diodes," Cambridge Studies in Semiconductor Physics and Microelectronic Engineering 2, Cambridge University Press, 1995.
• "NEMS devices," Nanoscale Silicon Devices, Taylor and Francis, pp. 123-154, CRD Press, 2015.

Membership in Academic Societies:
• Physical Society of Japan (PSJ)
• Japan Society of Applied Physics (JSAP)
• Electron Device Society of IEEE
• Institute of Physics (IOP), Fellow